

[FAAF][−] (A = O, S, Se, Te) or How Electrostatic Interactions Influence the Nature of the Chemical Bond

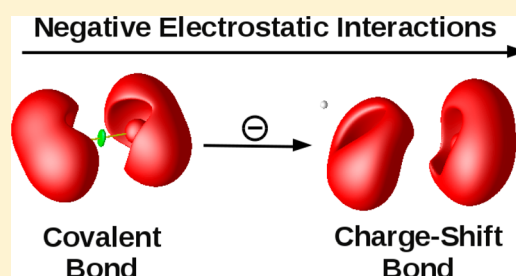
José A. Gámez^{†,*} and Manuel Yáñez[‡]

[†]Max-Planck-Institut für Kohlenforschung, Kaiser-Wilhelm-Platz 1, D-45470, Mülheim an der Ruhr, Germany

[‡]Departamento de Química, Módulo 13, Facultad de Ciencias, Universidad Autónoma de Madrid, Cantoblanco, ES-28049, Madrid, Spain

S Supporting Information

ABSTRACT: The present contribution analyzes the special bonding situation of the [FAAF][−] anions (A = O, S, Se, Te), where the addition on an extra charge turns the covalent A–A bond of the neutral into a charge-shift (CS) bond. By means of theoretical calculations, we demonstrate that electrostatic interactions produced by negative point charges can transform the covalent A–A bond in the A₂⁺ cation into a CS one. Consequently, the electric field created by the fluorine atoms can be behind the unusual bonding situation of [FAAF][−], showing how electrostatic interactions can influence and alter the nature of the chemical bond.



Chemical bonding is probably one of the most important and fundamental concepts in chemistry. The modern theory of chemical bonding was established with the pioneering paper by Lewis,¹ where he proposed the chemical bond as a consequence of electronic pairing, and was finally culminated in the classical book by Pauling.² According to this theory, molecules present two types of chemical bonds, namely covalent and ionic. Covalent bonds are due to the sharing of electronic density by two or more nuclei, increasing the electronic density in the bonding region with respect to the superimposed fragment densities. Ionic bonds, on the other hand, are stabilized by electrostatic interactions between ions of opposite charges. For more than 70 years, this paradigm has remained unchanged and has been able to successfully explain most of the chemical processes. However, more and more molecules have emerged whose bonding situations cannot be easily assigned to any of these two families.

The bonds H₃Si^{+0.85}F^{−0.85}, Li^{+0.94}F^{−0.94}, H₃Si^{+1.0}Cl^{−1.0}, and Na^{+0.91}Cl^{−0.91}, where the superscripts represent the charge of the groups obtained with a QTAIM analysis defining zero-flux surfaces in the gradient field of the electronic density and integrating the electronic density within such boundaries,³ all present an ionic charge distribution. However, while Li⁺F[−] and Na⁺Cl[−] behave as classical ionic compounds, Si⁺X[−] bonds show characteristics of covalent unions.⁴ In fact, although stable R₃C⁺ carbocations have been known for more than a hundred years, the first stable silylium ion was not crystallized until 2002, and since then, not many derivatives have been reported.⁵

Another striking example is the so-called depleted or protocovalent bonds, like F–F, Cl–Cl, O–O, or S–S.⁶ Experimentally, they are characterized by depleted or negative standard deformation densities in the bonding region,^{6a} contrary to the classical picture of covalent bonds where electronic density is accumulated in the bonding region to hold

the atoms together. Although deformation density measures suffer from an artificial choice of the reference protomolecule, theoretical estimates also confirm the depletion of electronic density for such molecules. Coherently, they present a positive Laplacian of the electronic density ($\nabla^2\rho$) at the bond critical point (bcp), and the cusp catastrophe of the bonding disynaptic basin $V(X,X')$ occurs for distances longer than the bond length,^{6b} which are characteristics of typical ionic bonds.⁷ Moreover, they present a covalent component of the wave function that is weakly bounding or even repulsive.^{3a} Shaik et al. found out that in such cases the bonding energy comes from the ionic-covalent fluctuation of the electron pair density,^{3a,8} the so-called charge-shift (CS) resonance energy (RE_{CS}). Challenging the model for the chemical bonding, they propose a new type of chemical bond, the CS bond, dominated by the RE_{CS} quantity, and different from conventional covalent and ionic bonds. CS bonds are found in linkages between atoms with a large number of electron lone pairs, like halogens or chalcogens. Consequently, while H–H is a true covalent bond, the F–F bond is a CS one. According to Shaik et al.,^{3a} Si–X bonds are also CS bonds, which would explain the aforementioned elusive formation of silylium ions. In contrast with carbocations, in silylium ions the positive charge is mainly borne by Si; hence, there is a tighter bond between silicon and the counterion than between carbon and its counterion. According to the arguments given in ref 3a, in the condensed phase the solvent stabilizes fewer silylium cations than carbocations, so the Si⁺–X[−] linkage still has a large RE_{CS} in the condensed phase. Since the heterolysis of the bond would result in the loss of the RE_{CS} energy, solvolysis must be necessarily difficult in silylium cations. The CS-bond concept

Received: March 27, 2013

also explains the unusual high barrier for halide-transfer reactions compared to the corresponding hydrogen-transfer process⁹ due to the loss of RE_{CS} energy in the reaction barrier. Indeed, CS bonds have become a topic of very active research and have been recently found in many diverse chemical situations.¹⁰

Our recent work on electron attachment to disulfides and diselenides¹¹ pointed out the special bonding situation of the $[FAAF]^-$ radical anions ($A = S, Se$). We showed that, due to symmetry, these systems can be described as a combination of two resonant forms: $^-FAAF \leftrightarrow FAAF^-$. The combination of those forms leads necessarily to a large fluctuation of the extra electron along the molecule, especially in the A–A bond. As mentioned above, electronic fluctuation is the key feature which binds the atoms together in CS bonds, and indeed, the A–A bonds in $[FAAF]^-$ show the characteristic fingerprints of such linkages:^{8a} disappearance of the $V(A,A)$ disynaptic basin of the Electron Localization Function (ELF),¹² large electronic fluctuation between the lone pair $V(A)$ monosynaptic basins (measured by the delocalization indexes $\delta(A,A')$ between the lone pairs monosynaptic basins), and a nearly zero value of $\nabla^2\rho$ at the A–A bcp. In contrast, in the neutral compounds, FAAF, the A–A bond is covalent as it is characterized by a $V(A,A)$ disynaptic basin of the ELF with a large population, low electronic fluctuation between the lone-pair monosynaptic basins^{7b} (see Table 1), and a large and negative value of $\nabla^2\rho$ at

Table 1. Population of the Lone-Pair Monosynaptic Basins for the A, $V(A)$, and F, $V(F)$, Atoms of the ELF Analysis for $[FAAF]^-$ ($[FAAF]^-$) ($A = S, Se$)^a

	$V(A,A)$	$V(A)$	$V(F)$	$\delta(A,A')$	$\delta(A,F)$
X = O	0.93	5.25 (5.99)	7.00 (7.13)	0.79 (0.42)	0.66 (0.87)
X = S	1.56	4.40 (5.75)	7.55 (7.43)	0.54 (1.72)	0.72 (0.62)
X = Se	1.41	4.70 (6.16)	7.58 (7.58)	0.58 (1.54)	0.66 (0.64)
X = Te	1.33	4.57 (5.68)	7.58 (7.65)	0.39 (1.00)	0.45 (0.46)

^aAlso displayed are the delocalization indexes between both A atoms, $\delta(A,A')$, and between A and F, $\delta(A,F)$. All values are in e and taken from ref 11b.

the bcp.^{7a} Therefore, the covalent A–A bond in the neutral FAAF turns into a CS bond in $[FAAF]^-$ due to the electronic fluctuation artificially produced by the extra electron roaming between both fluorine atoms. The present letter analyzes more in detail the bonding situation of these systems.

If one takes into account that, for $A = S$ and Se , the NBO analysis yields a rather large partial charge on both F atoms, namely -0.73 and $-0.69e$, respectively,^{11b} $[FAAF]^-$ could be regarded as a combination of A_2^+ with two fluoride anions. Under that assumption, the question would be, can the fluoride anions, by means of electrostatic interactions, be responsible for the particular bonding situation of $[FAAF]^-$? Or, in more general terms, may the interaction with point charges alter the nature of the A–A covalent bond? To answer that question, we have performed the following computational experiment: by using the optimized geometry of the $[FAAF]^-$ anion, we have analyzed the characteristics of the ELF when the two fluorine atoms are replaced by point charges of different value and sign.

The reference will be the A_2^+ cation, in which the A–A distance is that optimized for the $[FAAF]^-$ anion.

This study is extended also to O and Te, which represent two extreme cases in which the atoms involved in the bond have a high or a low electronegativity, respectively. FTeTeF behaves similarly to FSSF and FSeSeF: upon electron capture, the $V(Te,Te)$ disynaptic basin disappears and the electronic fluctuation between the lone pairs of tellurium increases dramatically (see Table 1). However, FOOF is substantially different. The neutral system presents a $V(O,O)$ disynaptic basin with already a small population ($0.93e$) and a high electronic fluctuation between the oxygen lone pairs, pointing out already to some CS character in the O–O bond of the neutral system. In the anion, the $V(O,O)$ basin disappears, but the delocalization index $\delta(O,O')$ also decreases, contrary to what was observed for the other systems. This observation suggests that the O–O in the $[FOOF]^-$ anion is not really a CS bond but a weak interaction between the OF subunits.¹¹ Indeed, FOOF, and hence its anion, is substantially different from the other FAAF analogues here considered.¹³ The O–O distance in the $[FOOF]^-$ anion is much larger (1.921 \AA) with respect to that of the neutral (1.216 \AA). This represents an elongation of the O–O of the neutral of 60%, while for the other molecules there is practically no elongation upon anion formation (1%, 3%, and 4% for $X = S, Se$, and Te , respectively). Indeed, O_2^+ presents no disynaptic basin either when its ELF is computed at an O–O distance of 1.921 \AA (see Supporting Information), which reinforces the idea that the O–O bond in $[FOOF]^-$ is not really a CS one but a weak interaction. In summary, for the oxygen derivative, the O–O bond is already a CS bond in the neutral and almost cleaves in the anion. Hence, in what follows we will restrict our analysis to S, Se, and Te.¹⁴

The results of this computational experiment for $A = Se$ are shown in Figure 1. Similar results are found for $A = S$ and Te .

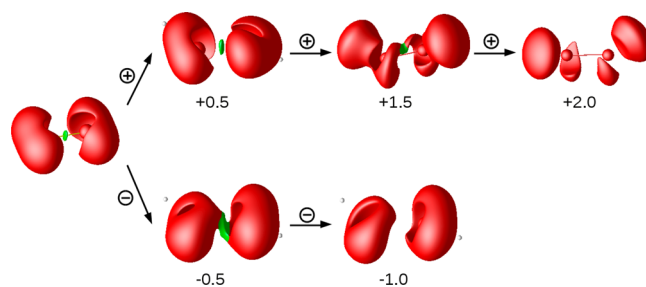


Figure 1. Localization domains of the ELF ($ELF = 0.75$) for Se_2^+ interacting with two point charges. The point charges are represented with small white balls. The value of the charges (in e) is displayed under each figure. Red lobes correspond to monosynaptic basins and those in green, to disynaptic basins.

The left side of the figure shows the isolated Se_2^+ , with two lone pairs on each Se and an elliptical disynaptic $V(Se,Se)$ basin, characteristic of a covalent double bond. This picture does not change significantly when two charges of $+0.5e$ are placed at the same positions as the two F atoms in the $[FAAF]^-$ structure. It is apparent that the lone pairs only get polarized toward the charges, whereas the disynaptic $V(Se,Se)$ basin is hardly perturbed. When the positive charge increases ($+1.5$), the lone pairs become more and more polarized, being closer and closer to the point charges than to the selenium atoms. To compensate for this depletion of electronic density in the valence region, the density at the internuclear region starts to

Table 2. Basin Population and Delocalization Indexes between the Lone Pair Monosynaptic $V(A)$ Basins of the ELF Analysis for the A_2^+ Cation, $A = S, Se, Te$, in the Presence of Different Point Charges^a

charge		0	+0.5	+1.0	+1.5	+2.5	−0.5	−1.0	−1.5	−2.5
$V(A,A)$	S	1.8177	1.7359	1.5937	1.6080		1.8524	0.8951		
	Se	1.4003	1.2128	1.1172	1.1219		0.6902			
	Te	1.7542	1.4045	0.8872			1.4949	1.1611	0.7298	
$V(A)$	S	4.5272	4.5615	4.6343	4.6315	3.1318	4.4992	4.9738	5.4146	5.5566
	Se	4.8950	4.9892	5.0339	5.0227	3.2651	5.2481	5.5833	6.0149	5.4924
	Te	4.6845	4.9302	5.2620	3.5273	3.4452	4.8699	5.0077	5.1780	5.3996
$\delta(A,A')$	S	0.8566	0.8608	0.8698	0.8022	0.3236	0.8456	1.2600	1.8606	1.8000
	Se	0.9978	0.9624	0.9060	0.7602	0.7544	1.2896	1.6868	1.6224	1.5342
	Te	0.4413	0.4883	0.5410	0.4935	0.5139	0.5316	0.6551	0.8817	1.1764

^aAll values in e.**Table 3. Potential Energy, $V(r)$, and Gradient Kinetic Energy, $G(r)$, Densities, and the Local Virial Ratio, $|V(r)|/G(r)$, Evaluated at the Bond Critical Point (bcp) for the A_2^+ Cation, $A = S, Se, Te$, in the Presence of Different Point Charges^a**

charge		0	+0.5	+1.0	+1.5	+2.5	−0.5	−1.0	−1.5	−2.5
$ V(r) /G(r)$	S	2.4707	2.4909	2.4992	2.4888	2.2814	2.4432	2.4127	2.3832	2.3370
	Se	2.1220	2.1314	2.1290	2.0819	1.8393	2.1045	2.0799	2.0529	2.0124
	Te	1.9290	1.9924	1.9311	1.8708	1.5946	1.9696	1.9299	1.8985	1.7079
$G(r)$	S	0.0759	0.0741	0.0721	0.0703	0.0742	0.0773	0.0785	0.0794	0.0806
	Se	0.0457	0.0439	0.0422	0.0420	0.0469	0.0473	0.0486	0.0499	0.0520
	Te	0.0263	0.0255	0.0256	0.0261	0.0254	0.0264	0.0270	0.0274	0.0280
$V(r)$	S	−0.1875	−0.1846	−0.1802	−0.1750	−0.1693	−0.1889	−0.1894	−0.1892	−0.1884
	Se	−0.0970	−0.0936	−0.0899	−0.0874	−0.0863	−0.0995	−0.1011	−0.1024	−0.1046
	Te	−0.0507	−0.0508	−0.0494	−0.0488	−0.0405	−0.0520	−0.0521	−0.0520	−0.0478

^aAll energy densities are in $E_h a_0^{-3}$, and point charges, in e.

migrate to the lone pairs of Se. If the charge is further increased (+2.0), some electronic density is localized around the point charges. As a result, the disynaptic $V(Se,Se)$ basin is finally destroyed and its population transferred to the $V(Se)$ ones in order to compensate for the polarization produced by the field created by point charges. The situation changes slightly, at least pictorially, when the charges placed at the positions of the fluorine atoms are negative. With charges of $-0.5e$, the lone pair monosynaptic $V(Se)$ basins fuse with the bonding disynaptic $V(Se,Se)$ one as the lone pairs are repelled from the point charges. If the charge is further increased in absolute value up to $-1.0e$, the disynaptic basin completely disappears, and the lone pairs move even farther away from the point charges.

Table 2 provides a more quantitative picture of the changes in the bonding situations presented in Figure 1. When the fluorine atoms are replaced by positive charges, neither the population of the disynaptic $V(A,A)$ nor the Se–Se (S–S) bonding are much affected by charges below $+1.5e$. However, when the charge is increased to $+2.0e$, the $V(Se,Se)$ basin disappears. For $A = S$, this is produced at a higher charge ($+2.5e$) as the orbitals of selenium are more diffuse and polarizable. Coherently, Te cannot hold its valence electrons so strongly due to its lower electronegativity. Hence, the disynaptic $V(Te,Te)$ basin disappears already for a positive charge of $+1.5e$. When the fluorine atoms are replaced by negative charges the population of this basin decreases much more rapidly but the mechanism behind this disappearance is totally different. As aforementioned, the electric field created by positive charges produces the depletion of the electronic density at the valence region of the molecule, which is compensated by density coming from the internuclear (bonding) region. It is also noteworthy that, for the A_2^+

systems, the delocalization index $\delta(A,A')$ remains more or less constant for positive charges. This picture is radically different under the influence of negative charges. In this instance, there is no depletion of electronic density but a significant increase of the interelectronic repulsion, which triggers an electron pair density fluctuation. Coherently, although the $V(A,A)$ basin eventually disappears, there is a concomitant and remarkable increase of the $\delta(A,A')$ delocalization index. Both effects, the disappearance of the $V(A,A)$ basin and the increase of the $\delta(A,A')$ index, are clear indications of the CS character of the A–A linkage. Actually, the delocalization index is approximately twice as large when the disynaptic basin disappears due to a negative charge than when the disynaptic basin is removed by a positive charge. These findings seem to confirm that electrostatic interactions with negative charges may transform a covalent bond, with high $V(A,A)$ populations and low $\delta(A,A')$, into a CS bond, with no $V(A,A)$ basins and high $\delta(A,A')$ values. This is not surprising, however, as CS bonds arise in situations where the covalent bonding mechanism is no longer efficient due to a high interelectronic repulsion.^{3a,8a} Indeed, with a highly negative charge, the interelectronic repulsion increases, and only the electron pair density fluctuation characteristic of CS bonds can account for the stabilization of the bond.

A QTAIM analysis was performed to further confirm this picture. Table 3 shows the potential energy density, $V(r)$, and the gradient kinetic energy density, $G(r)$, evaluated at the bond critical point (bcp). When the A–A bond interacts with both positive and negative point charges, the local virial ratio $|V(r)|/G(r)$ diminishes. This can result from either an increase of the potential energy density (decrease in absolute value as $V(r)$ is negatively defined) or an increase of the gradient kinetic energy density. For the case of positive charges, the increase of $V(r)$ is

larger than the increase of $G(r)$. As previously argued on the basis of ELF results, positive charges eventually remove electronic density from the bonding region, so the bonding interactions holding the atoms together become weaker. In such a case, the potential energy density should decrease, in absolute value, significantly. The QTAIM confirms this trend. On the contrary, under the effect of negative point charges, the increase of the gradient kinetic energy density overcomes the decrease of the potential energy density, as shown by the trend in $|V(r)|/G(r)$. Surprisingly, although the attractive interactions between the nuclei become stronger, as shown by the lowering of $V(r)$, the covalent bond does not survive. Indeed, the negative charges produce a contraction of the valence orbitals, consistent with a lower potential energy density but at the price of overshooting $G(r)$. Indeed, the CS-bond mechanism was proposed to explain those instances where, due to the orbital contraction inherent to the bond making process,¹⁵ the lowering in potential energy does not compensate for the dramatic increase of the kinetic energy.^{3a,8a} The QTAIM analysis shows, again, that a covalent bond behaves very similarly to a CS one when interacting with negative charges.

In conclusion, the present work reveals that the nature of a covalent bond can be significantly modified with an external negative point charge by enhancing the fluctuation of the electron pair density. The particular bonding situation of the $[FAAF]^-$ systems, with the A–A linkage being a CS bond, was previously explained in terms of the electronic fluctuation due to the extra electron roaming between both fluorines for symmetry constraints. The present analysis shows that a CS bond is also obtained considering a model with two negative charges interacting with the A–A bond. This opens up the question whether for other molecules the bonding situation may also be modified due to electrostatic interactions with negative charges as found in a crystalline ionic lattice.

■ COMPUTATIONAL METHODS

To better compare the bonding situations between $[FAAF]^-$ and A_2^+ interacting with point charges, the A–A bond distance of the former system (1.963, 2.279, and 2.711 Å for A = S, Se, and Te, respectively, at the CCSD/6-31+G(d) level of theory -LANL2DZdp for A = Te), is the one adopted in our survey. This is not much different from the optimized bond distance of A_2^+ (1.842 and 2.126 Å for A = S and Se, respectively, at the CCSD/6-31+G(d) level of theory, 2.519 Å for A = Te at the CCSD/LANL2DZdp level), and actually, the ELF analysis is quite similar using both bond lengths (see the Supporting Information). The ELF analysis is known to be dependent on the dynamical electronic correlation, especially in CS bonds and other so-called depleted covalent bonds,^{6b} so the CCSD/6-31+G(d) (LANL2DZdp for A = Te) level is chosen as a benchmark. However, the wave function of A_2^+ with point charges shows a high multireference character, so the CASSCF(11,10) method is chosen instead. In addition to this method, the Atomic Natural Orbitals basis set ANO-S[10s6p3d/6s5p3d] (for A = O), ANO-S[17s15p9d/7s6p3d] (for A = S), the Dunning one cc-aug-pVTZ (for A = Se), and ANO-RCC[22s19013d5f3g/9s8p7d4f1g] (for A = Te) give similar results to the CCSD/6-31+G(d) level (CCSD/ANO-RCC[22s19013d5f3g/7s6p4d2f1g] for A = Te; see Supporting Information). Consequently, in the main manuscript, only ELF analyses with CASSCF densities are presented. The population of some relevant ELF basins has been calculated as well as some of the delocalization indexes¹⁶ between basin pairs. For A = Te,

a scalar relativistic effect has been introduced through the Douglas–Kroll Hamiltonian when the full-electron ANO-RCC basis was utilized. To further confirm the ELF predictions, a complementary QTAIM analysis^{7a,17} has been performed with the aforementioned CASSCF densities. Precisely, the gradient kinetic energy density, $G(r)$, and the potential energy density, $V(r)$, have been evaluated at the bond critical point (bcp). The CCSD calculations were performed with the Gaussian 03 package of programs¹⁸ and the CASSCF ones with the MOLCAS7.4 program.¹⁹ The ELF analysis was performed with the DGrid 4.6²⁰ and Multiwfn²¹ programs.

■ ASSOCIATED CONTENT

Supporting Information

Optimized geometries for the $[FAAF]^-$ systems. Comparison between the ELF analysis undertaken with CCSD and CASSCF densities. Comparison between the ELF analysis on the A_2^+ system performed at the A_2^+ equilibrium bond distance and at the A–A bond distance in the $[FAAF]^-$ anion. ELF analysis of O_2^+ interacting with point charges. This information is available free of charge via the Internet at <http://pubs.acs.org>

■ AUTHOR INFORMATION

Corresponding Author

*E-mail: jgamez@kofo.mpg.de. Phone: +49 208 306 2171. Fax: +49 208 306 2996.

Notes

The authors declare no competing financial interest.

■ ACKNOWLEDGMENTS

This work has been partially supported by the DGI Projects No. CTQ2012-35513-C02-01. J.A.G. acknowledges the Alexander von Humboldt Stiftung for a postdoctoral fellowship. A generous allocation of computing time is also acknowledged to the CCC-UAM.

■ REFERENCES

- (1) Lewis, G. N. The atom and the molecule. *J. Am. Chem. Soc.* **1916**, 38, 762–785.
- (2) Pauling, L. *The Nature of the Chemical Bond*; Cornell University Press: Ithaca, NY, 1939.
- (3) (a) Shaik, S.; Danovich, D.; Silvi, B.; Lauvergnat, D.; Hiberty, P. Charge-Shift Bonding—A Class of Electron-Pair Bonds That Emerges from Valence Bond Theory and Is Supported by the Electron Localization Function Approach. *Chem.—Eur. J.* **2005**, 11, 6358–6371. (b) Bader, R. F. W.; Nguyen-Dang, T. T. Quantum Theory of Atoms in Molecules—Dalton Revisited. In *Advanced Quantum Chemistry*; Löwdin, P.-O., Ed.; Academic Press: New York, 1981; Vol. 14, pp 63–124.
- (4) Gibbs, G. V.; Boisen, M. B. A Molecular Modeling of the Bonded Interactions of Crystalline Silica. In *The Chemistry of Organic Silicon Compounds*; Rappoport, Z., Apeloig, Y., Eds.; John Wiley & Sons, Ltd: New York, 2003; pp 103–118.
- (5) (a) Apeloig, Y.; Stanger, A. The first demonstration of solvolytic generation of a simple silicenium ion (R_3Si^+). Access via 1,2-methyl migration. *J. Am. Chem. Soc.* **1987**, 109, 272–273. (b) Lambert, J. B.; Kania, L.; Zhang, S. Modern Approaches to Silylium Cations in Condensed Phase. *Chem. Rev.* **1995**, 95, 1191–1201. (c) Kim, K.-C.; Reed, C. A.; Elliott, D. W.; Mueller, L. J.; Tham, F.; Lin, L.; Lambert, J. B. Crystallographic Evidence for a Free Silylium Ion. *Science* **2002**, 297, 825–827.
- (6) (a) Coppens, P. *X-Ray Charge Densities and Chemical Bonding*; Oxford University Press: Oxford, U. K., 1997. (b) Llugar, R.; Beltrán, A.; Andrés, J.; Noury, S.; Silvi, B. Topological analysis of electron

density in depleted homopolar chemical bonds. *J. Comput. Chem.* **1999**, *20*, 1517–1526.

(7) (a) Bader, R. F. W. *Atoms in Molecules. A Quantum Theory*; Oxford Univ. Press: Oxford, U. K., 1990. (b) Silvi, B.; Savin, A. Classification of chemical bonds based on topological analysis of electron localization functions. *Nature* **1994**, *371*, 683–686.

(8) (a) Shaik, S.; Danovich, D.; Wu, W.; Hiberty, P. C. Charge-shift bonding and its manifestations in chemistry. *Nat. Chem.* **2009**, *1*, 443–449. (b) Wu, W.; Song, J.; Shaik, S.; Hiberty, P. Classification of chemical bonds based on topological analysis of electron localization functions. *Angew. Chem., Int. Ed.* **2009**, *121*, 1435–1438. (c) Zhang, L.; Ying, F.; Wu, W.; Hiberty, P.; Shaik, S. Topology of Electron Charge Density for Chemical Bonds from Valence Bond Theory: A Probe of Bonding Types. *Chem.—Eur. J.* **2009**, *15*, 2979–2989.

(9) Hiberty, P. C.; Megret, C.; Song, L.; Wu, W.; Shaik, S. Barriers of Hydrogen Abstraction vs Halogen Exchange: An Experimental Manifestation of Charge-Shift Bonding. *J. Am. Chem. Soc.* **2006**, *128*, 2836–2843.

(10) (a) Tian, Y.-H.; Kertesz, M. Charge Shift Bonding Concept in Radical π -Dimers. *J. Phys. Chem. A* **2011**, *115*, 13942–13949. (b) Jenkins, S.; Kirk, S. R.; Guevara-Garcia, A.; Ayers, P. W.; Echegaray, E.; Toro-Labbe, A. The mechanics of charge-shift bonds: A perspective from the electronic stress tensor. *Chem. Phys. Lett.* **2011**, *510*, 18–20. (c) Berski, S.; Latajka, Z.; Gordon, A. J. Electron Localization Function and Electron Localizability Indicator Applied to Study the Bonding in the Peroxynitrous Acid HOONO. *J. Comput. Chem.* **2011**, *32*, 1528–1540. (d) Berski, S.; Latajka, Z.; Gordon, A. J. Oxygen bound iodine (O-I): The Electron Localization Function (ELF) study on bonding in cis- and trans-IONO. *Chem. Phys. Lett.* **2011**, 50615–21. (e) Ploshnik, E.; Danovich, D.; Hiberty, P. C.; Shaik, S. The Nature of the Idealized Triple Bonds Between Principal Elements and the sigma Origins of Trans-Bent Geometries-A Valence Bond Study. *J. Chem. Theory Comput.* **2011**, *7*, 955–968. (f) Rzepa, H. S. The rational design of helium bonds. *Nat. Chem.* **2010**, *2*, 390–393. (g) Shaik, S.; Chen, Z.; Wu, W.; Stanger, A.; Danovich, D.; Hiberty, P. C. An Excursion from Normal to Inverted C-C Bonds Shows a Clear Demarcation between Covalent and Charge-Shift C-C Bonds. *ChemPhysChem* **2009**, *10*, 2658–2669. (h) Barbosa, A. G. H.; Barcelos, A. M. The electronic structure of the F_2 , Cl_2 , Br_2 molecules: the description of charge-shift bonding within the generalized valence bond ansatz. *Theor. Chem. Acc.* **2009**, *122*, 51–66. (i) Jubert, A.; Okulik, N.; Michelini, M. d. C.; Mota, C. J. A. Topological Insights into the Nature of the Halogen-Carbon Bonds in Dimethylhalonium Ylides and Their Cations. *J. Phys. Chem. A* **2008**, *112*, 11468–11480.

(11) (a) Gámez, J. A.; Yáñez, M. Asymmetry and Electronegativity in the Electron Capture Activation of the Se–Se Bond: $\sigma^*(\text{Se}–\text{Se})$ vs $\sigma^*(\text{Se}–\text{X})$. *J. Chem. Theory Comput.* **2010**, *6*, 3102–3112. (b) Gámez, J. A. *Electron Capture Dissociation of Disulphides and Diselenides*. Ph.D. Dissertation, Universidad Autónoma de Madrid, Madrid, Spain, 2011.

(12) Becke, A. D.; Edgecombe, K. E. A simple measure of electron localization in atomic and molecular systems. *J. Chem. Phys.* **1990**, *92*, 5397–5403.

(13) Prascher, B. P.; Wilson, A. K. A computational study of dihalogen- μ -dichalcogenides: XAAX ($\text{X} = \text{F}, \text{Cl}, \text{Br}$; $\text{A} = \text{S}, \text{Se}$). *J. Mol. Struct. (THEOCHEM)* **2007**, *814*, 1–10.

(14) The results of this computational experiment for $\text{A} = \text{O}$ can be found in the Supporting Information, confirming that in this case the behavior of oxygen is totally different from that of sulfur, selenium, or tellurium.

(15) Feinberg, M. J.; Ruedenberg, K. Paradoxical Role on the Kinetic-Energy Operator in the Formation of the Covalent Bond. *J. Chem. Phys.* **1971**, *14*, 1495–1511.

(16) Fradera, X.; Austen, M. A.; Bader, R. F. W. The Lewis Model and Beyond. *J. Phys. Chem. A* **1998**, *103*, 304–314.

(17) Matta, C. F.; Boyd, R. J. *The Quantum Theory of Atoms in Molecules*; Wiley-VCH: Weinheim, Germany, 2006.

(18) Frisch, M. J.; Trucks, G. W.; Schlegel, H. B.; Scuseria, G. E.; Robb, M. A.; Cheeseman, J. R.; Montgomery, J. A., Jr.; Vreven, T.; Kudin, K. N.; Burant, J. C.; Millam, J. M.; Iyengar, S. S.; Tomasi, J.;

Barone, V.; Mennucci, B.; Cossi, M.; Scalmani, G.; Rega, N.; Petersson, G. A.; Nakatsuji, H.; Hada, M.; Ehara, M.; Toyota, K.; Fukuda, R.; Hasegawa, J.; Ishida, M.; Nakajima, T.; Honda, Y.; Kitao, O.; Nakai, H.; Klene, M.; Li, X.; Knox, J. E.; Hratchian, H. P.; Cross, J. B.; Bakken, V.; Adamo, C.; Jaramillo, J.; Gomperts, R.; Stratmann, R. E.; Yazyev, O.; Austin, A. J.; Cammi, R.; Pomelli, C.; Ochterski, J. W.; Ayala, P. Y.; Morokuma, K.; Voth, G. A.; Salvador, P.; Dannenberg, J. J.; Zakrzewski, V. G.; Dapprich, S.; Daniels, A. D.; Strain, M. C.; Farkas, O.; Malick, D. K.; Rabuck, A. D.; Raghavachari, K.; Foresman, J. B.; Ortiz, J. V.; Cui, Q.; Baboul, A. G.; Clifford, S.; Cioslowski, J.; Stefanov, B. B.; Liu, G.; Liashenko, A.; Piskorz, P.; Komaromi, I.; Martin, R. L.; Fox, D. J.; Keith, T.; Al-Laham, M. A.; Peng, C. Y.; Nanayakkara, A.; Challacombe, M.; Gill, P. M. W.; Johnson, B.; Chen, W.; Wong, M. W.; Gonzalez, C.; Pople, J. A. *Gaussian 03*, revision D.01; Gaussian, Inc.: Pittsburgh, PA, 2004.

(19) (a) Aquilante, F.; De Vico, L.; Ferré, N.; Ghigo, G.; Malmqvist, P.-Å.; Neogrády, P.; Pedersen, T. B.; Pitoňák, M.; Reiher, M.; Roos, B. O.; Serrano-Andrés, L.; Urban, M.; Veryazov, V.; Lindh, R. MOLCAS 7: The Next Generation. *J. Comput. Chem.* **2010**, *31*, 224–247. (b) Veryazov, V.; Widmark, P.-O.; Serrano-Andrés, L.; Lindh, R.; Roos, B. O. MOLCAS as a development platform for quantum chemistry software. *Int. J. Quantum Chem.* **2004**, *100*, 626–635. (c) Karlström, G.; Lindh, R.; Malmqvist, P.-Å.; Roos, B. O.; Ryde, U.; Veryazov, V.; Widmark, P.-O.; Cossi, M.; Schimmelpennig, B.; Neogrady, P.; Seijo, L. MOLCAS: a program package for computational chemistry. *Comput. Mater. Sci.* **2003**, *28*, 222–239.

(20) Kohout, M. *DGrid*, version 4.6; Radebeul, Germany, 2011.

(21) Lu, T.; Chen, F. Multiwfn: A multifunctional wavefunction analyzer. *J. Comput. Chem.* **2012**, *33*, 580–592.